Article

Behavior of Autumn Airborne Ragweed Pollen and Its Size-Segregated Allergens (*Amb a 1*): A study in Urban Saitama, Japan

Weiqian Wang [1,*], Qingyue Wang [1,*], Senlin Lu [2], Yichun Lin [1], Miho Suzuki [1] and Yuma Saito [1]

1   Graduate School of Science and Engineering, Saitama University, 255 Shimo-Okubo, Sakura-ku, Saitama 338-8570, Japan
2   School of Environmental and Chemical Engineering, Shanghai University, 99 Shangda Road, Shanghai 200444, China
*   Correspondence: weiqian@mail.saitama-u.ac.jp (W.W.); seiyo@mail.saitama-u.ac.jp (Q.W.); Tel.: +81-48-858-3519 (W.W.); +81-48-858-3733 (Q.W.)

Abstract: The prevalence of ragweed (*Ambrosia artemisiifolia*) pollinosis has been increasing worldwide. This study focused on the behavior of autumn airborne pollen and the major ragweed allergen -*Amb a 1* particle in urban Saitama, Japan, in 2016. Burkard sampler results showed that the airborne ragweed pollen scattering season was from September 1st to October 9th. Over 83% of sampling events had pollen counts of over 13 grains/m^3, indicating the high potential health risks of ragweed pollen in the atmosphere. The results of a surface plasmon resonance immunoassay (SPR) indicated that the average *Amb a 1* count was about 16.5 pg /pollen. The airborne *Amb a 1* concentration was up to 4.7 ng/m^3, of which about 45% was accumulated in ultrafine particles, such as particulate matter with a diameter ≤ 1.1 μm (PM$_{1.1}$). Although ragweed pollen was hardly observed during the October 14th–17th sampling campaign, the concentration of ambient *Amb a 1* particles in PM$_{1.1}$ was also determined to be 4.59 ng/m^3, which could be explained by the longer scattering of fine particles in the atmosphere. Pearson correlation coefficient analysis results showed that temperature (daily, r = 0.41; event, r = 0.87) could affect the behavior of the airborne pollen counts, and ambient water-soluble ions (such as Ca^{2+} and NO$_3{}^-$) could affect *Amb a 1* in PM$_{1.1}$. Additionally, air mass trajectories and wind rose results indicated that air masses with long-range transportation could also influence the temporary behavior of *Amb a 1* and pollen counts via the wind. Mugwort and *Humulus japonicus* pollens were also observed to extend pollen scattering periods. Airborne pollen and allergenic particles could be considered air pollutants, as they pose health risks and are susceptible to environmental influences.

Keywords: *Amb a 1*; fine particles; ionic contents; ragweed pollen; SPR analysis; Japan

1. Introduction

Pollinosis is reportedly caused by pollen from various botanical species. Ragweed (*Asteraceae* family) pollen has been considered to be the main cause of pollinosis and asthma since the 1930s [1]. According to the Asthma and Allergy Foundation of America, in 2002, ragweed allergy affected around 30% of Americans, and it can even trigger asthma symptoms [2]. In Europe, the primary report of ragweed pollen sensitization was conducted in the 1980s [3]. For example, ragweed sensitization rates have been reported to be as high as about 47% in France and up to 60% in Hungary, where the treatment costs for ragweed allergy are about EUR 100 million per year [4]. Meanwhile, in Asia, the situation seems to be a little different, with only around 5% of the population being sensitive to ragweed pollen [4]. In Japan, ragweed pollen is considered the second most common source of pollen allergies after *Cryptomeria* [1]. Additionally, 23.7% of patients with ragweed pollen allergies also show asthma symptoms, which could be considered another indicator of

the allergenic potency of ragweed [3]. The Kanto area has the largest city economy in the world and is a major global center for trade, as well as the center of Japan. The population is over 40 million, accounting for about one-third of the nation's population (https://www.japan.go.jp/regions/kanto.html, accessed on 1 January 2017). Tokyo had a higher hay fever prevalence of 28.2% in 2006 [5].

Ragweed pollen is a significant aeroallergen, the grain of which is only 15–25 μm in diameter and the surface of which is covered in short pines [3,6,7]. The major ragweed allergens from the *Amb a 1* to *Amb a 11* group have been identified and described. *Amb a 1* is an acidic non-glycosylated protein (38kDa) with 397 amino acids, which belong to the pectatelyase protein family [8]. *Amb a 1* also has a 58% sequence homology with the Art v 6 allergen from mugwort, and it is a better T-cell stimulant [4]. Generally, the allergenic content of pollen is identified and quantified using the enzyme-linked immunosorbent assay (ELISA) method [9–11]. Recently, the surface plasmon resonance (SPR) immunoassay method has been increasingly applied in the protein research area [12–14]. The SPR system can measure biomolecular interactions in real-time with a high sensitivity, and it has allowed for the generation of important kinetic information to determine the strength of binding interactions between antibodies [15]. In the pollen allergenic area, Gong used the SPR method to identify airborne *Cry j 1* and *Cry j 2* (from *Cryptomeria japonica*) in Saitama, Japan [12,13]. It has also been reported that meteorological and environmental factors can affect the behavior of airborne pollen and allergenic particles [13,14]. For example, ragweed pollen production is stimulated by an increase in atmospheric CO_2 [2,16]. Moreover, the generation of allergen particles from *Japanese cedar* pollen occurs after exposure to high humidity, rainwater, or polluted urban air [14]. Ionic contents (Ca^{2+}, NH_4^+, and SO_4^{2-}) could aggravate pollen rupture and content release, and they could affect allergenic *Pla a 3* in ambient particles. The Ca^{2+} ions in yellow sand are considered to be important factors affecting the release of allergenic *Cry j 1* [13]. In terms of aerodynamic diameter, allergenic pollen particles, such as $PM_{2.5}$, can increase allergenicity by inducing allergic asthma.

This study principally focused on the characteristics of autumn airborne pollen and the *Amb a 1* aeroallergen in the Saitama area of the Kanto region, Japan. The details are as follows: (1) we collected airborne pollen using classic Burkard and rotary samplers and collected ambient particles using a high-volume Andersen-type air sampler from a representative area in Saitama; (2) we identified the pollen species and determined the pollen counts using an optical microscope, determined the ambient *Amb a 1* concentration using the SPR method, and measured the ionic compounds using ion chromatography (IC); (3) we explored the temporal distributions of the pollen and *Amb a 1* concentrations; and (4) we evaluated the influences of meteorological and environmental factors on the pollen and allergenic particles in the atmosphere. From this research, we aimed to obtain information about the aerial distribution of pollen in autumn, which could provide some important insights into how to improve the control of pollinosis.

2. Materials and Methods

2.1. Airborne Pollen and Allergenic Particle Sampling in Saitama

The sampling site (Figure 1a–c) was located in the Saitama City Arakawa Sports Park, which is the largest local park in Saitama, with an area of about 25,698 m² and about 184,000 annual users (2016) (https://www.city.saitama.jp/006/013/001/005/p059378.html, accessed on 1 January 2017). We identified different kinds of herbaceous plants in the study area, including *Ambrosia psilostachya* (ragweed), *Ambrosia trifida* (giant ragweed), *Artemisia princeps* (mugwort), and *Humulus japonicus* (Japanese hop).
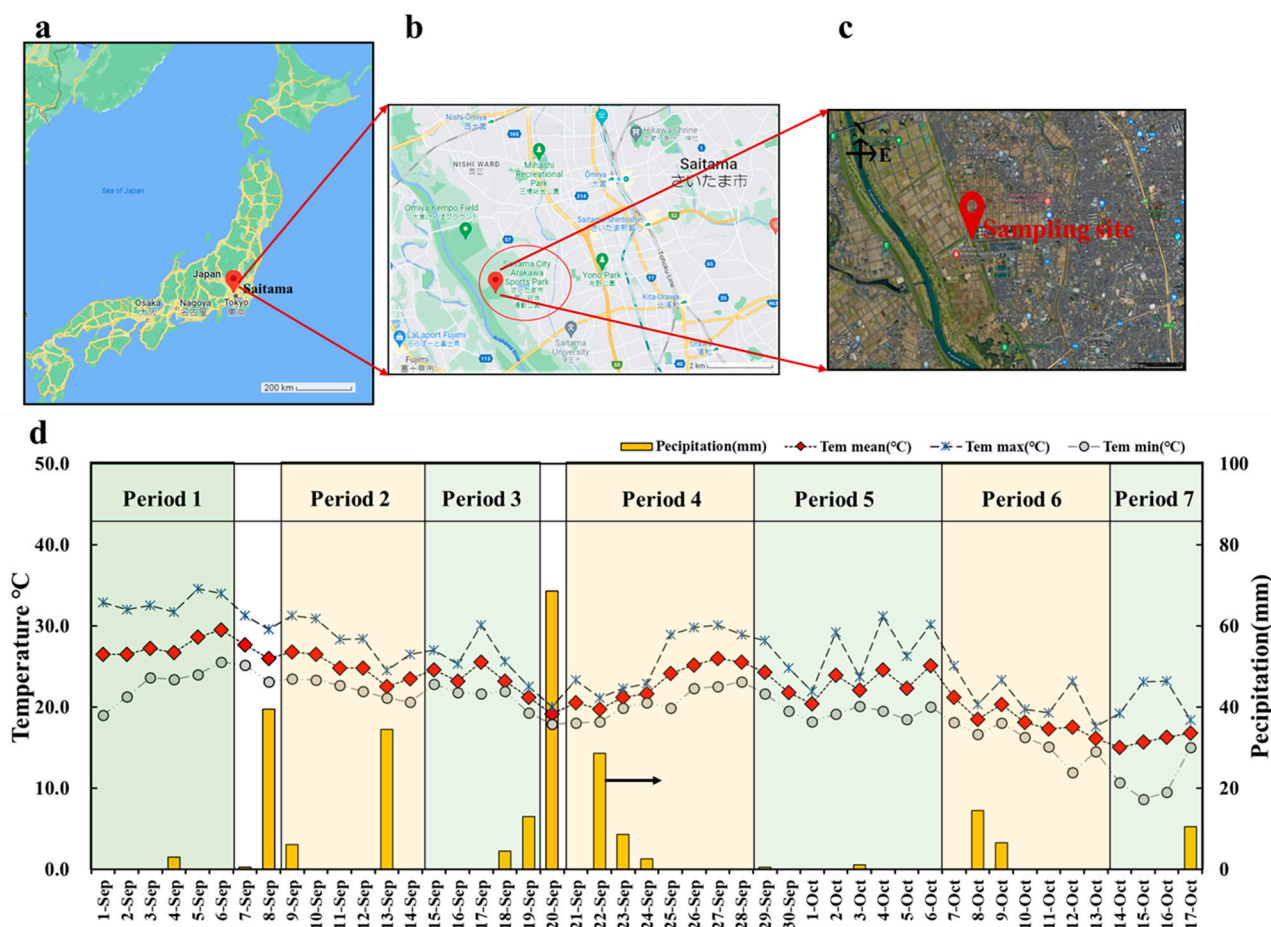
Figure 1. (**a**) The location of Saitama City in Japan; (**b**,**c**) the location of the sampling sites in the park. These images are from Google Maps. (**d**) The mean, maximum, and minimum temperatures and the precipitation levels over the total sampling period.

The airborne pollen sampling campaign was conducted using a Burkard (Hirst-type) 7-day recording volumetric spore trap (Burkard Manufacturing Co. Ltd., Rickmansworth, UK) and a rotary pollen sampler (RK-1SA, Nishiseiki Co., Ltd., Kitakyushu, Japan). Burkard (Hirst-type) volumetric spore traps are a type of volumetric pollen sampler, and they are the standard pollen monitors widely used in Europe and the United States [9]. Our pollen sampling periods were from September 1st to October 17th, 2016, excluding rainy and stormy days (such as September 7th, 8th, and 20th). Airborne pollen grains were collected over 24 h using the rotary sampler, which was changed at AM9:00 JST. Ambient particles with five size-segregated stages were collected using an Andersen-type high-volume air sampler (AHV-600, Sibata scientific technology Co., Ltd., Saitama, Japan) with a 566 L/min airflow. A characteristic of this sampler is that it can collect ambient particles in five size-segregated stages to simulate the human respiratory system. Ambient particles were collected on quartz fiber filters (2500 QAT-UP, Tokyo Dylec Co., Ltd., Kyoto, Japan) and divided into these 5 stages as follows: $PM_{1.1}$, which can pass through the alveoli into the circulatory system; $PM_{1.1-2.0}$, which can pass through the bronchial branches; $PM_{2.0-3.3}$, which can pass into the bronchium; $PM_{3.3-7.0}$, which can be retained in the bronchial branches, the pharynges, and the throat; and PM with a diameter above 7.0 μm (coarse particles), which can be retained in the mouth and nasal cavity. The total sampling periods were spilt into seven periods as follows: September 1st–6th (period 1); September 9th–14th (period 2); September 15th–19th (period 3); September 21st–28th (period 4); September 29th–October 6th (period 5); October 7th–13th (period 6); and October 14th–17th (period 7).

Simultaneously, during this 2016 ambient sampling campaign, meteorological data were collected from the Saitama City Ward Office, which was the nearest atmospheric sampling site; these data were obtained by the Japan Meteorological Agency using an automated meteorological data acquisition system (accessed on December 9th, 2016). The environmental data were collected from a continuous air pollution monitoring system in Saitama Prefecture (accessed on December 6th, 2016). The measurement factors were as follows: temperature (°C), relative humidity (RH), precipitation (mm), daily sunlight (h), wind direction (WD), and wind speed (WS) (m/s), as well as individual measurements of $PM_{2.5}$, SPM, SO_2, and NOx (as shown in Figure 1d and Table S1).

2.2. Observation of Airborne Pollen and Counting Statistics

The physical characteristics of the collected pollen were measured using a scanning electron microscope (SEM) (SU1510, HITACHI, Hitachi, Japan), as shown in Figure 2. The airborne pollen samples were stained using a Phöbus Blackly distain solution (0.6 mg of methyl violet 2B, 60 mL of ethanol, 30 mL of phenol, 180 mL of glycerol, and 90 mL of ultrapure water) [12,14], and they were then counted using an optical microscope (GLB-B1500MBITaN, Shimadzu RIKA Co. Ltd., Tokyo, Japan). The pollen counts collected by the Burkard sampler were calculated in the unit of pollen grains/m^3. The airborne pollen counts collected by the rotary sampler were calculated in the unit of pollen grains/cm^2.
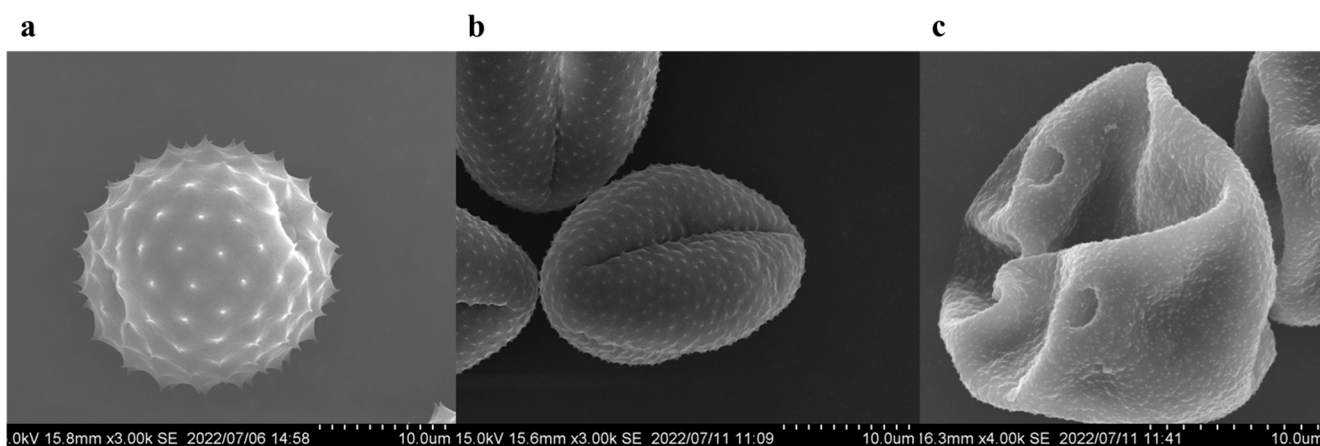

Figure 2. Physical characteristics of pollen measured using an SEM microscope, with an accelerating volage of 15.0 kV and a length of 16.3 mm, and SE image edition: (**a**) ragweed pollen, (**b**) mugwort, (**c**) *Humulus japonicus*.

2.3. Determination of Amb a 1 Concentration Using the SPR Method

To extract the allergenic content, the following process was used: sampling filters were cut into 20 pieces of 8 mmφ; 1.5 mL of extracting buffer (150 mM of NaCl, 125 mM of NH_4HCO_3, 3 mM of EDTA, 0.005% (*v/v*) Tween 20, and 10mM of HEPES) was added, and the mixture was incubated at 4 °C for 24 h; the floating particles were removed via centrifugation at 6000× *g* rpm for 30 min; then, 500 μL of the supernatants was added to the centrifugal filter units (Amicon®Ultra 0.5, Millipore Co., Ltd., Tokyo, Japan) in order to exchange the solvent for an initial volume of 450 μL of HBS-EP buffer (BR-1001-88, GE Healthcare Co., Ltd., Chicago, IL, USA) to make 500 μL; and, finally, the *Amb a 1* concentration was measured using a BIACORE J system (GE Healthcare Co., Ltd., Tokyo, Japan), based on the SPR method [12–14]. The details of the method are as follows: the surface of the SA sensor chip (BR-1003-98, GE Healthcare Co., Ltd., Tokyo, Japan) was cleaned with three consecutive 1 min injections of 1 M of NaCl (191-01665, Wako Pure Chemical Industries, Ltd., Osaka, Japan) in 50 mM of NaOH (BR-1003-58, GE Healthcare Co., Ltd., Tokyo, Japan); immobilization was performed using an HBS-EP buffer (N_2 gas purge-degassed) at a medium flow rate (30 μL/min) at 25 °C; the ragweed *Amb a 1* IgG antibody (INDOOR Biotechnologies, Inc., Cardiff, UK) was bound to the SA sensor chip

using the capturing method via the high-affinity binding between biotin and streptavidin (Avidin/Biotin Blocking Kit, Thermo Scientific, Waltham, MA, USA); and the biotinylated antibody was diluted 1/200-fold in the HBS-EP buffer and coupled for 5 min on the sensor surface until the immobilization level reached saturation at 3000 resonance units (RU) (3.0 ng/mm^2).

After the immobilization of the biotinylated antibody using the capturing method, a calibration curve was drawn for the binding of the *Amb a 1* standard solution (Natural Amb a 1, NA-AAR1, INDOOR Biotechnologies, Inc., UK). The *Amb a 1* standard line was measured at concentrations of 0, 12.5, 25, 50, 100, 200, and 300 ng/mL using triplicate measurements. The analysis was performed at 25 °C in HBS-EP (N$_2$ gas purge-degassed) at a medium flow rate (30 µL/min). The bound analyte was removed from the sensor chip surface after each allergen sample was injected with 5 M of NaCl in the HBS-EP buffer or 10 mM of glycine–HCl, pH 2.5, for 1–2 min until the RU signal decreased to the baseline. The SPR analysis was repeated using this regeneration procedure. Finally, the atmospheric *Amb a 1* allergen concentration could be calculated as follows:

$$C = \frac{(Ms - Mb) \times E \times S}{s \times V} \tag{1}$$

where *C* is the target content concentration (ng/m^3) contained in the particulate matter, Ms is the target content analysis value (ng/mL) of the sample test solution, Mb is the target content analysis value (ng/mL) of the sample blank solution, E is the constant volume of the test solution (mL), S is the filter area (cm^2) for collecting ambient particle samples, s is the filter area (cm^2) for the test solution, and V is the collection amount (m^3).

2.4. Determination of Water-Soluble Ions and pH in Ambient Particles

Eight species of water-soluble ions (Na$^+$, Ca^{2+}, NH$_4^+$, K$^+$, Mg^{2+}, Cl$^-$, SO$_4^{2-}$, and NO$_3^-$) in the ambient particles were analyzed using liquid chromatography (Aquion and Dionex ICS-1600, Thermo Fisher Scientific Co., Waltham, MA, USA). The details of the analysis are presented in our previous publications [11,17,18]. The pH values of the water-soluble solutions were measured using a pH meter (LAQUAtwin, Ph-11B, Horiba Co., Kyoto, Japan). The ionic concentrations in the atmosphere could be calculated as above in Equation (1), and they are shown in Table S2.

2.5. Analysis of Backward Air Mass Trajectories and Data Statistics

The hybrid single-particle Lagrangian integrated trajectory (HYSPLIT) model [17–19] is a computer model that is used to simulate air mass trajectories in order to determine how far and in what direction air and, subsequently, air pollutants can travel [19]. The HYSPLIT model is also capable of calculating the dispersion, chemical transformation, and deposition of air pollutants. The HYSPLIT model was selected to create a database of backward air mass trajectories using data from the global data assimilation system (GDAS) on the web server of the National Oceanic and Atmospheric Administration (NOAA) Air Resources Laboratory. The data statistics were collated using Microsoft Excel 2019 and Origin 2018 software.

3. Results

3.1. Temporary Characterization of three Airborne Herbaceous Pollen

Our observations of the airborne pollen that was collected using the Burkard sampler are shown in Figure 3. Ragweed pollen was undoubtedly the most dominant pollen between September 1st and October 9th. The peak of ragweed pollen, with 312 pollen grains/m^3, occurred on September 1st. Simultaneously, the results obtained using the rotary sampler also showed that the peak day of ragweed pollen occurred on September 4th, with 105 pollen grains/cm^2. For the total sampling campaigns, a Pearson correlation coefficient (PCC) analysis showed very strong correlations (r = 0.83, *p* < 0.001) between the pollen counts collected by these two pollen samplers, indicating the evidenced reality

pollen's temporary behaviors. Hence, the peak period of ragweed pollen could be delimited as the beginning of September in 2016. In addition to ragweed pollen, Figure 3b shows that ambient mugwort pollen was present from September 12th to October 13th, although the counts were under 11 grains/m³. Figure 3c shows that the average *Humulus japanious* pollen count was about 14.3 (1–54) grains/m³, and this kind of pollen could be observed at the end of the entire sampling period.
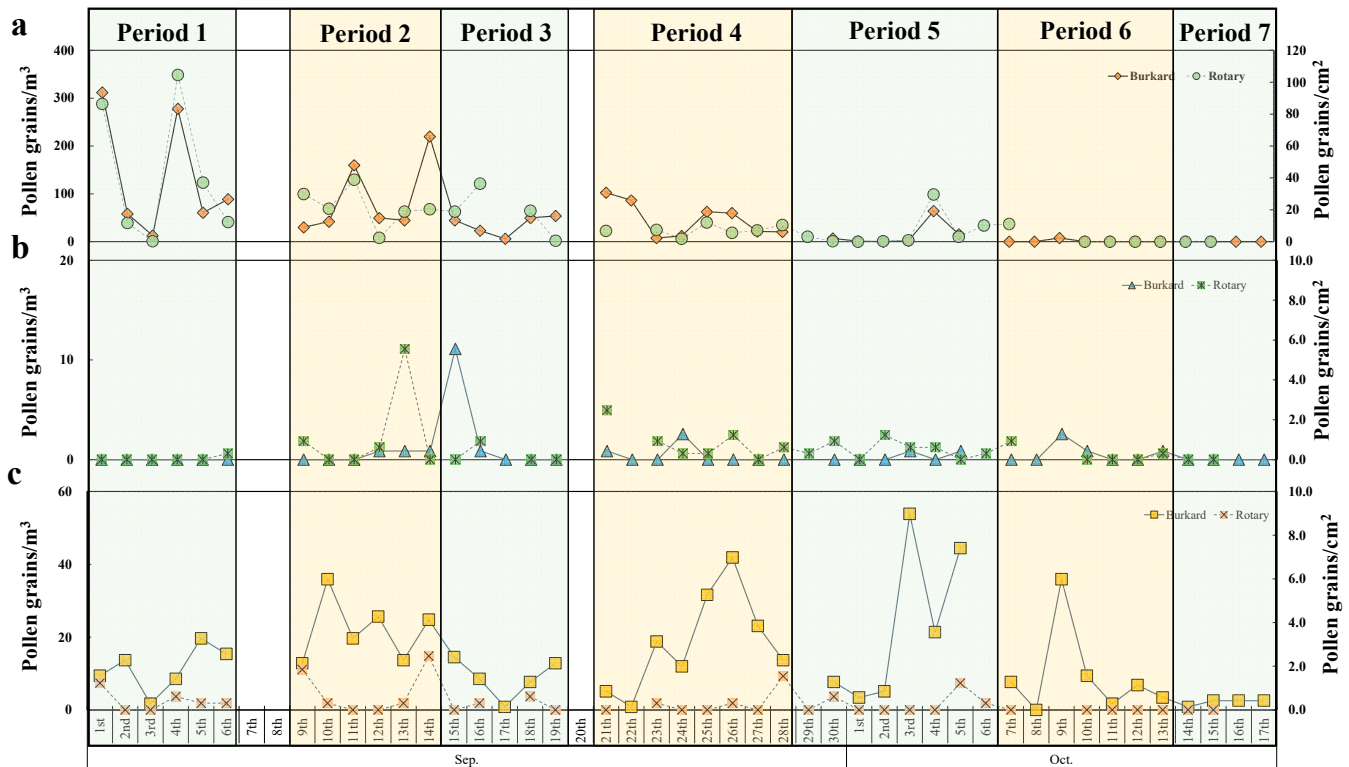

Figure 3. The temporal characterization of airborne herbaceous pollen, as measured using Burkard and rotary samplers: (**a**) ragweed; (**b**) mugwort; (**c**) *Humulus japonicus*.

3.2. The Effects of Meteorological and Environmental Factors on the Airborne Dispersion of Ragweed Pollen

The influences of meteorological factors on the dispersion of airborne pollen counts are normally observed using the Pearson correlation coefficient (PCC) [14,20]. Our PCC (Table 1) results indicated that, during the ragweed pollen scattering period, temperature had a positive effect on the airborne ragweed pollen count (mean, r = 0.41; maximum, r = 0.39; and minimum, r = 0.33; *p* < 0.05). The principal component analysis (PCA) results (Table S3) also indicated that the temperature factor could be considered the dominant positive factor affecting pollen count, while the humidity factor might have some negative effects. Otherwise, two representative sampling campaigns (such as September 4th with 278 pollen/m³ and September 3rd with 13 pollen/m³) were selected to observe the potential air mass long-distance transportation and wind effects. As shown in Figure 4a, the air mass backward trajectories on September 4th mainly came from the southern area, and they mainly came from more eastern area on September 3rd. The wind rose, as shown in Figure 4b, indicated that the wind on September 4th mainly came from the mild NNW (north-northwest) direction and the strong SSW (south-southwest) direction, while that on September 3rd mainly came from the eastern area.
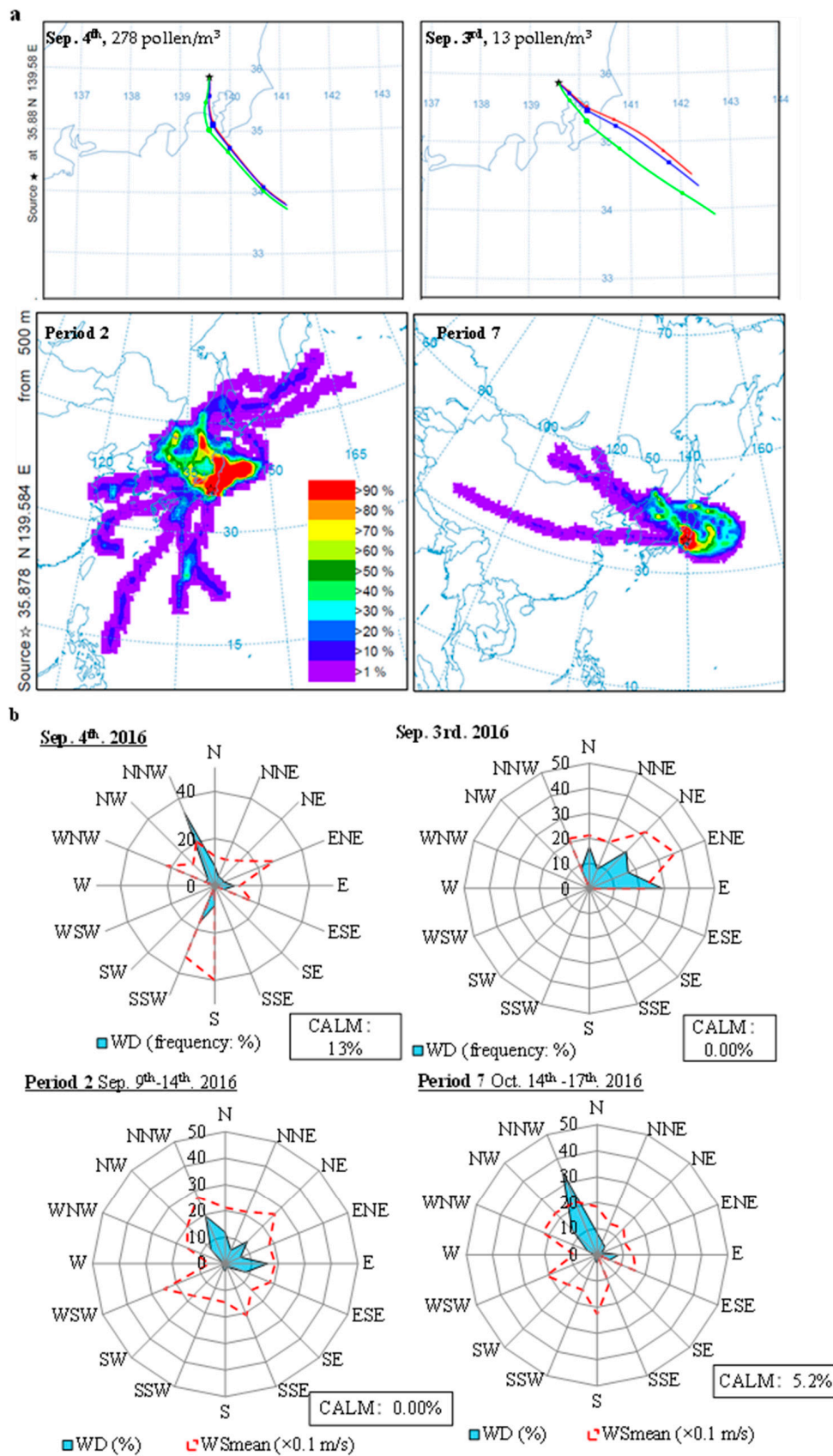
Table 1. Results of Pearson correlation coefficient between ragweed pollen, *Amb a 1*, and meteorological parameters and air pollutants.

| | | Ragweed (Burkard) | | Ambient *Amb a 1* | | |
		Daily	**Event**	**TSP**	**PM$_{1.1}$**	**Coarse Particles**
Ragweed (Burkard)	Daily	1	—	—	—	—
	Event	—	1	−0.53	−0.58	−0.38
Ragweed (Rotary)		**0.83**				
	TSP	—	−0.53	1	**0.88**	**0.77**
Amb a 1	PM$_{1.1}$	—	−0.58	**0.88**	1	**0.93**
	Coarse particles		−0.38	**0.77**	**0.93**	1
Temperature mean (°C)		0.41	**0.87**	−0.52	−0.73	−0.58
RHmean (%)		0.07	0.17	−0.72	−0.58	−0.42
Daily sunlight (h)		0.160	0.36	0.58	0.47	0.52
Precipitation (mm)		—	−0.03	−0.52	−0.37	−0.21
WSmean (m/s)		0.03	0.24	0.24	0.12	−0.29
PM$_{2.5}$ mean			−0.42	0.58	0.74	0.70
	Ca^{2+}	—	—	0.66	**0.87**	**0.99**
PM$_{1.1}$	NO$_3^-$	—	—	0.58	**0.82**	**0.90**
	K$^+$	—	—	0.41	0.62	0.54
	Mg^{2+}	—	—	0.49	0.64	**0.79**
	Ca^{2+}	—	—	**0.93**	**0.91**	**0.77**
Coarse particles	NO$_3^-$	—	—	−0.04	−0.37	−0.57
	K$^+$	—	—	−0.32	−0.45	−0.66
pH		—	—	—	**−0.64**	

boldface, $p < 0.05$.

3.3. Size and Temporal Distributions of Amb a 1 in the Atmosphere

During all of the seven sampling periods, the average airborne *Amb a 1* concentration in the total suspended particles (TSP) was about 4.71 ng/m^3, and it was always in the range of 2.25–7.90 ng/m^3, as shown in Figure 5 and Table S4. Table 2 also shows that the seasonal cumulative Amb a 1 concentration was high (33.0 ng/m^3) and was distributed as follows: about 45.2 % was in PM$_{1.1}$, 14.5 % was in PM$_{1.1–2.0}$, 13.0% was in PM$_{2.0–3.3}$, 14.2% was in PM$_{3.3–7.0}$, and 13.1% was in coarse particles. It was observed that *Amb a 1* was primarily distributed in ultrafine particles, such as PM$_{1.1}$ and PM$_{1.1–2.0}$. Table 1 demonstrates that the ambient *Amb a 1* concentration had a strong positive correlation with that in PM$_{1.1}$ (r = 0.82, $p < 0.05$) and in coarse particles (r = 0.62, $p = 0.19$). In terms of the temporal distribution, the highest *Amb a 1* concentration in the TSP was 7.90 ng/m^3, which occurred during period 7 (October 14th–17th), while the lowest was 2.25 ng/m^3, which occurred during period 2 (September 9th–14th). In particular, from period 5 onward, the *Amb a 1* concentration increased, and the concentrations were over 5 ng/m^3. Moreover, Table 2 shows that the average *Amb a 1* per pollen was approximately 16.5 pg/pollen.
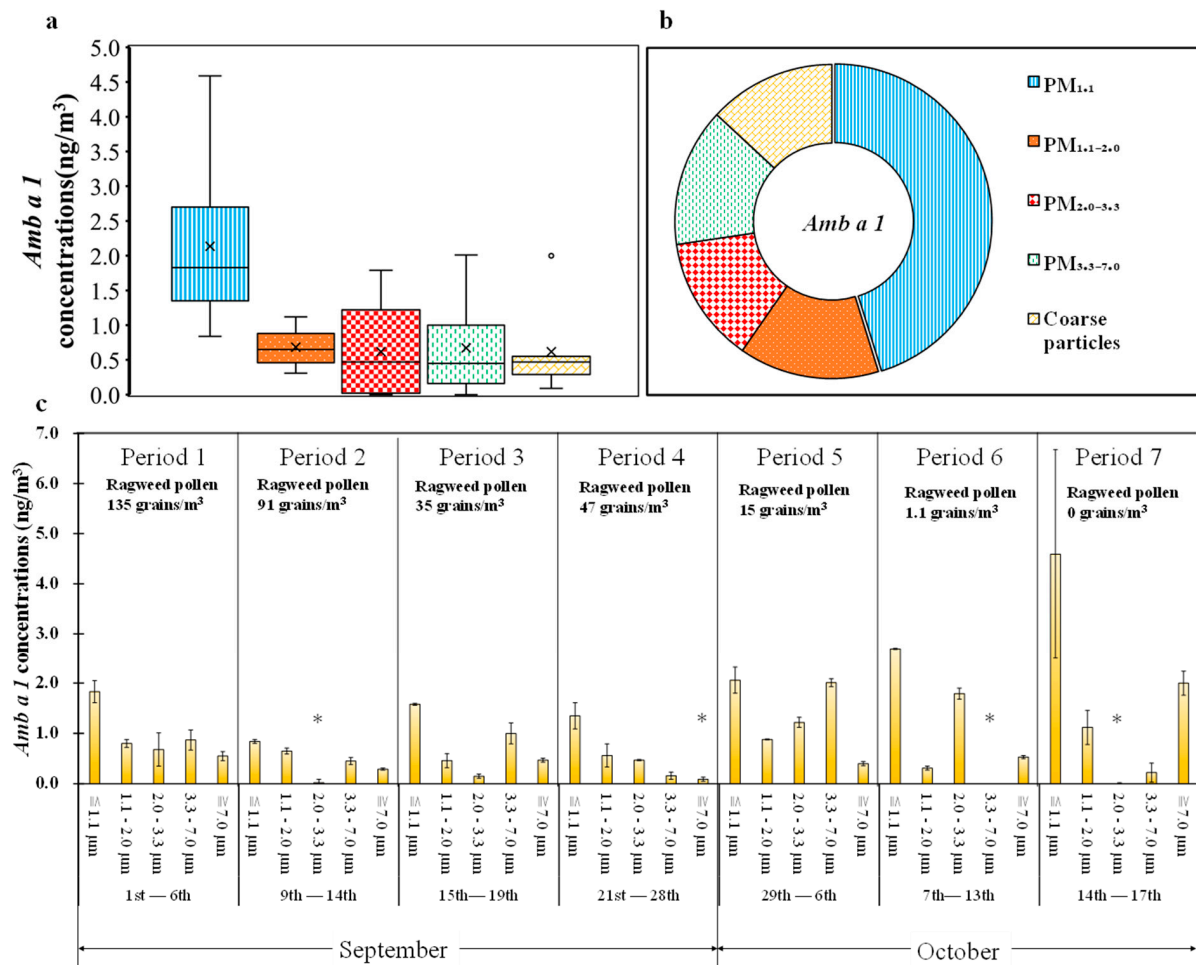
Figure 4. (**a**) The air mass trajectories on September 4th and September 3rd; period 2 and period 7; (**b**) the wind roses and directions on September 4th and September 3rd event; period 2 and period 7.

Figure 5. (**a**) The size distribution of *Amb a 1* in ambient particles; (**b**) the percentage of *Amb a 1* in ambient particles; (**c**) the temporal and size distributions of *Amb a 1* in ambient particles during each sampling period.

Table 2. The ambient ragweed pollen and *Amb a 1* allergen and preceding weather parameters for Saitama, 2016.

	2016
Pollen Scattering	
Peak daily ragweed pollen count (pollen/m^3)	**312**
Peak day	**September 1st**
Cumulative seasonal ragweed pollen count (pollen/m^3)	**2002**
Amb a 1	
Maximum *Amb a 1* concentration (ng/m^3)	**7.9**
Cumulative seasonal *Amb a 1* concentration (ng/m^3)	**33.00**
Peak event	**P7 (October 13th–17th)**
Average *Amb a 1* per pollen (pg/pollen)	**16.5**
Temperature (°C)	
Average daily	**22.7**
Average daily max.	**29.5**
Average daily min.	**15**
Relative Humidity	
Average daily (%)	**70.6**

3.4. Influences of Environmental Factors on Amb a 1 Distribution

As shown in Table 1, our PCC results showed that the ambient *Amb a 1* concentration in the TSP demonstrated a strong positive correlation with the *Amb a 1* concentration in $PM_{1.1}$ (r = 0.88) and coarse particles (>7.0 μm) (r = 0.77). Therefore, as a representative air pollutant, the water-soluble ionic content of these two-stage ambient particles was selected to demonstrate their potential impacts on allergen behavior. As shown in Figure 6, compared to that in coarse particles, the NH_4^+ and SO_4^{2-} ionic contents in $PM_{1.1}$ were high, and the Na^+, Ca^{2+}, Cl^-, and NO_3^- ionic contents were chiefly accumulated in coarse particles (>7.0 μm). Table 1 also shows that the *Amb a 1* concentration in $PM_{1.1}$ had a strong positive relationship with the Ca^{2+} (r = 0.87; $p < 0.05$) and NO_3^- (r = 0.82; $p < 0.05$) ions in $PM_{1.1}$, as well as with the Ca^{2+} (r = 0.91; $p < 0.05$) ions in coarse particles. Meanwhile, the *Amb a 1* concentration in coarse particles (>7.0 μm) also had a strong positive relationship with the Ca^{2+} (r = 0.77; $p < 0.05$) ions in coarse particles (>7.0 μm), as well as with the NO_3^- (r = 0.90; $p < 0.05$), Ca^{2+} (r = 0.99; $p < 0.01$), and Mg^{2+} (r = 0.79; $p < 0.05$) ions in $PM_{1.1}$. The *Amb a 1* concentration in the TSP could influence the daily mean $PM_{2.5}$ concentration (r = 0.58). Table 1 shows some of the factors that could potentially impact airborne *Amb a 1*, including temperature (mean, r = −0.52), relative humidity (mean, r = −0.72), daily sunlight (r = −0.58), precipitation level (r = −0.51), and $PM_{2.5}$ concentration (mean r = 0.57). Additionally, two typical sampling events were selected to demonstrate the potential effect of long-range air mass transportation on *Amb a 1* (i.e., period 2 with the lowest *Amb a 1* concentration in the TSP and period 7 with the highest *Amb a 1* concentration in the TSP). As shown in Figure 4, the air masses during period 2 came mainly from the northern and eastern directions, while the air masses during period 7 came mainly from the western and northern directions. Figure 4b shows that the wind roses for these two periods also had similar tendencies.
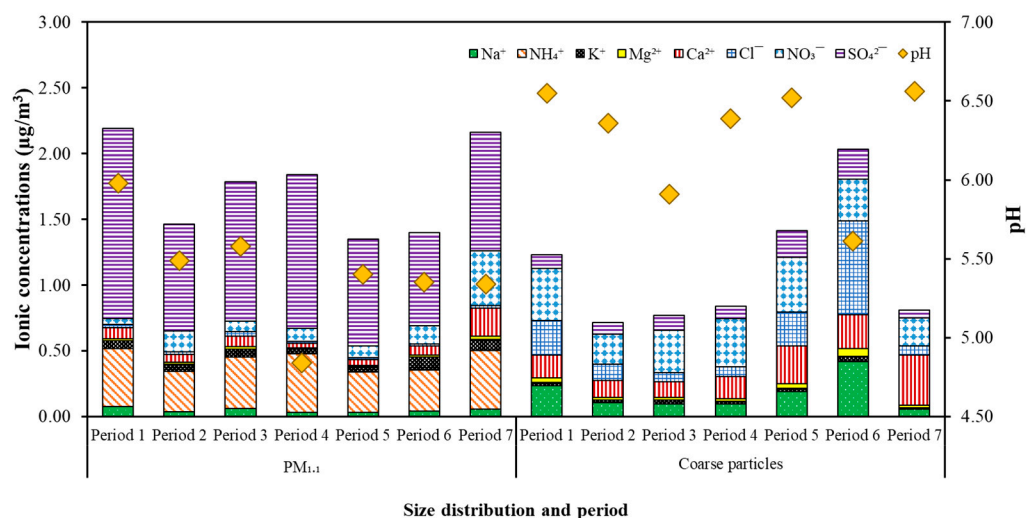

Figure 6. Distributions of water-soluble ionic contents and pH in $PM_{1.1}$ and coarse particles (>7.0 μm) during 7 sampling periods.

4. Discussion

4.1. The Behavior of Autumn Airborne Ragweed Pollen

According to Figure 3 and Table 2, the ambient ragweed pollen scattering season could be considered to be from September 1st to October 9th, with an average of 64 grains/m³ [21,22]. Generally, the threshold value of clinical symptoms of ragweed pollinosis is considered to be 13–30 pollen grains/m³, and a higher daily pollen count (>50 grains/m³) could increase the number of emergency department presentations for asthma attacks [22]. Among the 53 ambient ragweed pollen events during our sampling period (Figure 3), there were 15 events with pollen counts of over 50 grains/m³, which mostly occurred in September. Moreover, there were 44 sampling events with pollen counts over 13 grains/m³, indicating

the high potential health risk from ambient ragweed pollen. As the initial event had the highest count (312 pollen grains/m^3), the ragweed pollen dispersal period could be considered as being longer than the sampling period (September 1st–October 9th). Several other studies have focused on ragweed pollen all over the world. For example, a study conducted by Berger counted the ragweed pollen scattering season in Vienna (Austria) and determined that it occurred from August 26th to September 14th in 2016 [16]. In Zonguldak in Turkey, the pollen season was considered to be from August 30th to September 20th in 2015 and from July 28th to September 20th in 2016 [9], while the peak day occurred at the end of August, that is, August 30th in 2015 and August 25th in 2016 [9]. There was another study conducted in Turkey by Celenk, which presented that the ragweed pollen season in Bursa (Turkey) occurred from about August 3rd to September 22th in 2014 [19]. Our group also studied the airborne ragweed pollen in Saitama to identify whether the pollen scattering periods were similar across the last 4 years (data not shown). In brief, it seems that the ragweed pollen scattering season at these similar latitudes in the northern hemisphere mainly occurs from the end of August to the end of September. This inference could provide some important references around the world, especially in places where the ragweed pollen issue is not yet a concern.

Additionally, it should be mentioned that the pollen from mugwort and *Humulus japonicus* also possesses important characteristics that cannot be ignored. Moreover, all these three pollen species have long and overlapping dispersion periods, indicating that the sources and composition of autumn ambient pollen are diverse and persistent. In Szczecin in Poland, Malgorzata studied the ragweed and mugwort pollen from 2000 to 2003 and found that the mugwort pollen season had higher counts and was longer lasting than the ragweed pollen season [23]. Celenk found that mugwort pollen was also present during the ragweed pollen season [24]. Jeong reported that *Humulus japonicus*, sagebrush, and ragweed could be considered the major pollen producers in Korea during the September weed pollen season [25]. In this study, there were 20 events with pollen counts of over 13 grains/m^3, indicating that *Humulus japonicus* is an important pollen source.

In terms of the potential impacts of meteorological factors on pollen dispersal, our PCC results (Table 1) indicated that temperature influenced airborne ragweed pollen during the pollen scattering season. The PCA analysis (Table S3) also indicated that temperature was an important positive factor for pollen counts, while humidity had a negative effect. Peternal also presented a positive statistically significant correlation between airborne ragweed pollen counts and temperature factors [7,26]. Further, it has been reported that airborne pollen can be transferred by long-distance transportation from one area to another area [2,9,24]. The backward air mass trajectories on September 4th (278 pollen grains/m^3) mainly came from the southern direction, while those on September 3rd (13 pollen grains/m^3) came more from the eastern direction. The wind roses showed that there was mainly mild NNW wind and strong SSW wind on September 4th, while there was mainly eastern wind on September 13th. This could have been because the southern sampling site is surrounded by parks and farmland, whereas the eastern and northern sites are in densely populated residential areas. Long-distance transportation effects have also been conjectured based on local source effects [9,19,24]. In this study, temperature, humidity, wind, and even long-range transportation affected the airborne pollen counts. Therefore, it is necessary to find out more about the behavior of pollen and allergenic particles in the atmosphere.

4.2. Airborne Amb a 1 Distributed in Fine Particles

As is already known, it is essential to measure the ambient *Amb a 1* concentration in five size-segregated distributions when using the SPR method. Our results (Figure 5) show that *Amb a 1* particles were mainly distributed in ultrafine particles, especially in PM$_{1.1}$, which could be explained by the fact that one giant ragweed pollen grain can generate up to 1400 sub-pollen particles (SPPs) that are 0.018–6.5 um in size and 400 SPPs that are 0.6–6.5 um in size [27]. Generally, PM$_{1.1}$ is fine enough to pass through the alveoli into

the circulatory system and induce more potential health risks [14]. The highest *Amb a 1* concentration occurred during period 7, when ragweed pollen was hardly observed. Period 2 with 91 pollen grains/m^3 (Table S3) was observed to have the lowest *Amb a 1* concentration (2.25 ng/m^3). Our PCC results (Table 1) also demonstrated that there were no significant correlations between the pollen count and *Amb a 1* concentration. Gelenk also presented a similar extended period of ambient *Amb a 1* in Bursa in Turkey, and the average seasonal *Amb a 1* per pollen was about 2.57 pg/pollen [19], while a single plant could release about 1 billion pollen grains in a season [2]. Similar results have also appeared in a study on airborne *Cryptomeria japonica* pollen counts and *Cry j 2* allergens in Japan during 2012, with the results showing that higher *Cry j 2* concentrations occurred on March 16th–17th, while the pollen counts were very low [12].

Otherwise, ambient *Cry j 1* and *Cry j 2* have been measured using SPR in Saitama in Japan, indicating that the higher *Cry j 1* and *Cry j 2* concentrations were detected in PM$_{1.1}$ with ng/m^3 [12]. Zhou determined the ambient *Pla a 3* concentration in Shanghai using ELISA and found that it mostly existed in coarse particles, and intact *Platanus* pollen and non-negligible partitions of *Pla a 3* were detected in particles with diameters of less than 7.0 μm. In the study conducted in Zonguldak between 2015 and 2016, the ambient *Amb a 1* particles measured using ELISA were found to be up to 8.42 pg/m^3 and 13.1 pg/m^3, respectively, and *Amb a 1* in PM > 10 was found to be about 10 times higher than that in 10 > PM > 2.5 [9]. Grewling also reported the concentration of *Amb a 1* in Bursa in 2011 to be about 937.8 pg/m^3, and the concentrations in PM > 10 stages were about 10 times higher than that in 10 > PM > 2.5 [10]. In this study, the concentrations obtained using SPR and ELISA varied by a factor of about 10, which could be explained by their principal differences; for example, SPR produces optical results that are obtained directly from the reactions between antigens and antibodies.

4.3. Potential Environmental Influence Analysis of Pollen and Amb a 1

In recent decades, it has been proven that pollen allergens can be carried by fine particles (such as those with diameters of 2–5 um), for example, botanical fragments and bio-particulate [27]. When exposed to a high humidity and thunderstorms, pollen grains in the atmosphere are engorged with water and osmotically rupture to release sub-pollen particles (SPPs) [14]. SPPs have been detected in ambient particles; they are much smaller than the diameter of intact pollen and can reach deeper into the respiratory system to induce allergenic asthma. The highest *Amb a 1* concentration in our sampling period occurred during period 7, when almost no ragweed pollen was observed, which could be explained by the effects of grass-mowing events and cross-reactivity between *Amb a 1* and *Art v 6*. Our PCC results indicated that the Ca^{2+} in PM$_{1.1}$ and coarse particles had a strong positive impact on *Amb a 1* in both these two-stage particles. NO$_3{}^-$, which mainly accumulated in PM$_{1.1}$, also displayed a strong positive effect on *Amb a 1* in PM$_{1.1}$. Ca^{2+} is usually considered to be an indicator of sand particles, and NO$_3{}^-$ is a typical second particle, mainly from vehicle emissions [13,17]. Simultaneously, the air mass back trajectories showed that the air mass came from over the China area and passed through the western mountains, which are abundant with pollen, to the sampling site during period 7. The ionic contents in PM$_{1.1}$ during period 7 were at their higher concentrations, which also indicates the possible long-range transportation.

Furthermore, intact airborne pollen that is no longer detectable has spurred studies to explore the behavior of aeroallergens in submicronic particles, presumably from fragmented pollen grains. Fine particles likely react with urban air pollutants and denature chemically with their long detention time. It is well-known that pollen, as a source of pollen allergens, is influenced by various factors, for example, wind, air pollutants, and other species of pollen. Further attention should be paid to the effects of these factors on pollen and its allergenic particles.

5. Conclusions

To the best of our knowledge, this study is the first to focus on the airborne autumn pollen and allergen (*Amb a 1*) particles in an urban area in Japan. We observed pollen from different ragweed species, as well as pollen from mugwort and *Humulus japonicus*. The ragweed pollen scattering period was considered to be from early September to October, which was longer than the sampling campaign. We found that temperature, wind speed and direction, and long-range air mass transportation could impact pollen behavior. Higher *Amb a 1* concentrations, as determined using the SPR method, were found in ultrafine particles, even in $PM_{1.1}$, which can induce allergic asthma. Furthermore, these ambient fine allergenic particles can remain in the atmosphere for longer than pollen grains. Moreover, pollen allergenicity can be increased by atmospheric ionic contents via long-range air mass transportation in urban atmospheres. We considered pollen, pollen allergens, and atmospheric pollutants to not be independent within the atmosphere but rather a composite whole that could react with and influence each other. Therefore, studies on the mechanisms between these components are urgently needed. The health risks from autumn herbaceous pollinosis are considerable, not only in Japan but also in other Asian countries with overgrowths of these plant species. In this study, we proposed that an effective countermeasure for autumn herbaceous pollinosis could be weed management. Earlier weed-cutting campaigns could be used to control the living environments of plants. In further studies, it is necessary to supply more detailed information on autumn pollen counts and allergen concentrations, especially regarding the release of allergenic particles. Furthermore, pollinosis should be considered as a potential future social issue in some developing Asian countries.

6. Patents

There is no patent resulting from the work reported in this manuscript.

Abbreviations

PCC	Pearson correlation coefficient
CO_2	Carbon dioxide
EDTA	Ethylenediaminetetraacetic acid
ELISA	Enzyme-Linked Immunosorbent Assay
GDAS	Global Data Assimilation System
HEPES	4-(2-hydroxyethyl)-1-piperazineethanesulfonic acid
HYSPLIT	Hybrid Single Particle Lagrangian Integrated Trajectory
IC	Ion chromatography
NADPH	Nicotinamide adenine dinucleotide phosphate
NNW	North-northwest
NOAA	National Oceanic and Atmospheric Administration
PCA	Principal component analysis
PCC	Pearson correlation coefficient
PM	Particulate matter
$PM_{1.1}$	Fine particles with a diameter of 1.1 μm or less
$PM_{1.1-2.0}$	Fine particles with the particle sizes from 1.1 μm to 2.0 μm
$PM_{2.0-3.3}$	Fine particles with the particle sizes from 2.0 μm to 3.3 μm
$PM_{2.5}$	Fine particles with the particle sizes equal and below 2.5 μm
$PM_{3.3-7.0}$	Fine particles with the particle sizes from 3.3 μm to 7.0 μm
RU	Resonance unit
SCC	Spearman correlation coefficient
SEM	Scanning electron microscope
SPM	Suspended particulate matter
SPPs	Sub-pollen particles
SPR	Surface plasmon resonance
SSW	South-southwest
TSP	Total suspended particulate
WD	Wind direction
WS	Wind speed

References

1. Makra, L.; Matyasovszky, I.; Hufnagel, L.; Tusnady, G. The history of ragweed in the world. *Appl. Ecol. Environ. Res.* **2015**, *13*, 489–512.
2. Matthew, L.; Oswalt, G.D. Ragweed as an Example of Worldwide Allergen Expansion. *Allergy Asthma Clin. Immunol.* **2008**, *4*, 130–135. [CrossRef]
3. Turkalj, M.; Banic, I.; Anzic, S.A. A review of clinical efficacy, safety, new developments and adherence to allergen-specific immunotherapy in patients with allergic rhinitis caused by allergy to ragweed pollen (Ambrosia artemisiifolia). *Patient Prefer. Adherence* **2017**, *11*, 247. [CrossRef]
4. Chen, K.W.; Marusciac, L.; Tamas, P.T.; Valenta, R.; Panaitescu, C. Ragweed pollen allergy: Burden, characteristics, and management of an imported allergen source in Europe. *Int. Arch. Allergy Immunol.* **2018**, *176*, 163–180. [CrossRef] [PubMed]
5. Horii, M. Why do the Japanese wear masks? *Electron. J. Contemp. Jpn. Stud.* **2014**, *14*, 8.
6. Harrington, J.B., Jr.; Metzger, K. Ragweed pollen density. *Am. J. Bot.* **1963**, *50*, 532–539. [CrossRef]
7. Peternel, R.; Čulig, J.; Hrga, I.; Hercog, P. Airborne ragweed (*Ambrosia artemisiifolia* L.) pollen concentrations in Croatia, 2002–2004. *Aerobiologia* **2006**, *22*, 161–168.
8. D′amato, G.; Spieksma, F.T.M.; Liccardi, G.; Jäger, S.; Russo, M.; Kontou-Fili, K.; Nikkels, B.W.H.; Bonini, S. Pollen-related allergy in Europe. *Allergy* **1998**, *53*, 567–578. [CrossRef]
9. Alan, Ş.; Sarışahin, T.; Acar Şahin, A.; Kaplan, A.; Pınar, N.M. An assessment of ragweed pollen and allergen loads in an uninvaded area in the Western Black Sea region of Turkey. *Aerobiologia* **2019**, *36*, 183–195. [CrossRef]
10. Grewling, Ł.; Bogawski, P.; Jenerowicz, D.; Czarnecka-Operacz, M.; Šikoparija, B.; Skjøth, C.A.; Smith, M. Mesoscale atmospheric transport of ragweed pollen allergens from infected to uninfected areas. *Int. J. Biometeorol.* **2016**, *60*, 1493–1500. [CrossRef] [PubMed]
11. Zhou, S.; Zhao, H.; Peng, J.; Hong, Q.; Xiao, K.; Shang, Y.; Lu, S.; Zhang, W.; Wu, M.; Li, S.; et al. Size distribution of Platanus acerifolia allergen 3 (Pla a3) in Shanghai ambient size-resolved particles and Its allergenic effects. *Atmos. Environ.* **2019**, *198*, 324–334. [CrossRef]
12. Gong, X.; Wang, Q.; Lu, S.; Suzuki, M.; Nakajima, D.; Sekiguchi, K.; Miwa, M. Size distribution of allergenic Cry j 2 released from airborne Cryptomeria japonica pollen grains during the pollen scattering seasons. *Aerobiologia* **2016**, *33*, 59–69. [CrossRef]

13. Wang, Q.; Gong, X.; Suzuki, M.; Lu, S.; Sekiguchi, K.; Nakajima, D.; Miwa, M. Size-segregated allergenic particles released from airborne Cryptomeria japonica pollen grains during the Yellow Sand events within the pollen scattering seasons. *Asian J. Atmos. Environ.* **2013**, *7*, 191–198. [CrossRef]

14. Wang, Q.; Morita, J.; Gong, X.; Nakamura, S.; Suzuki, M.; Lu, S.; Sekiguchi, K.; Nakajima, T.; Nakajima, D.; Miwa, M. Characterization of the physical form of allergenic Cry j 1 in the urban atmosphere and determination of Cry j 1 denaturation by air pollutants. *Asian J. Atmos. Environ.* **2012**, *6*, 33–40. [CrossRef]

15. Rich, R.L. Higher-throughput, label-free, real-time molecular interaction analysis. *Anal. Biochem.* **2007**, *361*, 80018663136. [CrossRef] [PubMed]

16. Berger, M.; Bastl, K.; Bastl, M.; Dirr, L.; Hutter, H.P.; Moshammer, H.; Gstöttner, W. Impact of air pollution on symptom severity during the birch, grass and ragweed pollen period in Vienna, Austria: Importance of O(3) in 2010–2018. *Environ. Pollut.* **2020**, *263*, 114526. [CrossRef]

17. Wang, Q.; Wang, W. Size characteristics and health risks of inorganic species in PM1. 1 and PM2. 0 of Shanghai, China, in spring, 2017. *Environ. Sci. Pollut. Res.* **2020**, *27*, 14690–14701.

18. Wang, W.; Zhang, W.; Dong, S.; Yonemachi, S.; Lu, S.; Wang, Q. Characterization, pollution sources, and health risk of ionic and elemental constituents in PM2.5 of wuhan, central China. *Atmosphere* **2020**, *11*, 760.

19. Celenk, S. Detection of reactive allergens in long-distance transported pollen grains: Evidence from Ambrosia. *Atmos. Environ.* **2019**, *209*, 212–219. [CrossRef]

20. De Linares, C.; Belmonte, J.; Canela, M.; de la Guardia, C.D.; Alba-Sanchez, F.; Sabariego, S.; Alonso-Pérez, S. Dispersal patterns of Alternaria conidia in Spain. *Agric. For. Meteorol.* **2010**, *150*, 1491–1500. [CrossRef]

21. Erbas, B.; Jazayeri, M.; Lambert, K.A.; Katelaris, C.H.; Prendergast, L.A.; Tham, R.; Parrodi, M.J.; Davies, J.; Newbigin, E.; Abramson, M.J.; et al. Outdoor pollen is a trigger of child and adolescent asthma emergency department presentations: A systematic review and meta-analysis. *Allergy* **2018**, *73*, 1632–1641. [CrossRef] [PubMed]

22. Puc, M.; Wolski, T.; Camacho, I.C.; Myszkowska, D.; Kasprzyk, I.; Grewling, L.; Nowak, M.; Weryszko-Chmielewska, E.; Piotrowska-Weryszko, K.; Chlopek, K.; et al. Fluctuation of birch (Betula L.) pollen seasons in Poland. *Acta Agrobot.* **2015**, *68*, 303. [CrossRef]

23. Puc, M. Ragweed and mugwort pollen in Szczecin, Poland. *Aerobiologia* **2006**, *22*, 67–78. [CrossRef]

24. Marco, M.; Paola, D.M.; Alfonso, C.; Marzia, O.; Simone, O. Long distance transport of ragweed pollen as a potential cause of allergy in central Italy. *Ann. Allergy Asthma Immunol.* **2006**, *96*, 86–91.

25. Jeong, K.Y.; Han, I.S.; Choi, S.Y.; Lee, J.H.; Lee, J.S.; Hong, C.S.; Park, J.W. Allergenicity of recombinant profilins from Japanese hop, Humulus japonicus. *J. Investig. Allergol. Clin. Immunol.* **2013**, *23*, 345–350.

26. Majeed, H.T.; Periago, C.; Alarcón, M.; Belmonte, J. Airborne pollen parameters and their relationship with meteorological variables in NE Iberian Peninsula. *Aerobiologia* **2018**, *34*, 375–388. [CrossRef]

27. Stone, E.A.; Mampage, C.B.; Hughes, D.D.; Jones, L.M. Airborne sub-pollen particles from rupturing giant ragweed pollen. *Aerobiologia* **2021**, *37*, 625–632. [CrossRef]